



Rheological mechanical properties and its constitutive relation of soft rock considering influence of clay mineral composition and content

Xuebin Li¹ · Xuesheng Liu^{1,2} · Yunliang Tan^{1,2} · Ai Chen³ · Honglei Wang⁴ · Xin Wang¹ · Shenglong Yang¹

Received: 7 June 2023 / Revised: 23 July 2023 / Accepted: 28 July 2023
© The Author(s) 2023

Abstract

Rheological mechanical properties of the soft rock are affected significantly by its main physical characteristics-clay mineral. In this study, taking the mudstone on the roof and floor in four typical mining regions as the research object, firstly, the clay mineral characteristic was analyzed by the X-ray diffraction test. Subsequently, rheological mechanical properties of mudstone samples under different confining pressures are studied through triaxial compression and creep tests. The results show that the clay mineral content of mudstone in different regions is different, which leads to significant differences in its rheological properties, and these differences have a good correlation with the content of montmorillonite and illite-montmorillonite mixed layer. Taking the montmorillonite content as an example, compared with the sample with 3.56% under the lower stress level, the initial creep deformation of the sample with 11.19% increased by 3.25 times, the viscosity coefficient and long-term strength decreased by 80.59% and 53.94%, respectively. Furthermore, based on the test results, the damage variation is constructed considering the montmorillonite content and stress level, and the M–S creep damage constitutive model of soft rock is established. Finally, the test results can be fitted with determination coefficients ranging from 0.9020 to 0.9741, which proves that the constitutive relation can reflect the influence of the clay mineral content in the samples preferably. This study has an important reference for revealing the long-term stability control mechanism of soft rock roadway rich in clay minerals.

Keywords Clay mineral · Physical characteristic · Creep · Damage · Constitutive model

1 Introduction

With the increasing depletion of coal resources in the central and eastern regions of China, coal mining is gradually concentrated in the western regions such as Shanxi, Shaanxi,

Inner Mongolia, and Xinjiang (Xie et al. 2019; Yin et al. 2022). Most rocks belong to geological or high geo-stress soft rock produced by the special diagenetic environment and sedimentary process in the western region (Sun et al. 2019; Zhao et al. 2020; Tan et al. 2021), and usually contain more clay minerals, such as kaolin, montmorillonite, etc. (Liu et al. 2018; Sun et al. 2021; Jin et al. 2013), which makes the rock show rheological characteristics. From a macro point of view, the low long-term stability and high repair rate of roadway surrounding rock have become a major problem restricting the safe and efficient mining of coal resources in western regions.

Most of the current studies focus on the rheological properties of soft rock. For example, in terms of test, Chen et al. (2021) obtained the creep characteristics of sandy mudstone by the triaxial creep test, and the main parameters for controlling creep deformation were pointed out. Liu et al. (2020) obtained the macro and micro creep characteristics of soft rock by conducting the triaxial and nanoindentation creep test. Montero-Cubillo et al. (2021) obtained the creep failure characteristics of anchored soft rock through the pull-out

✉ Xuesheng Liu
xuesheng1134@163.com

✉ Yunliang Tan
yunliangtan@163.com

¹ College of Energy and Mining Engineering, Shandong University of Science and Technology, Qingdao 266590, China

² State Key Laboratory of Mining Disaster Prevention and Control, Shandong University of Science and Technology, Qingdao 266590, China

³ Ningxia Coal Industry Co., Ltd., of China Energy Group, Yinchuan 750000, China

⁴ Badong National Observation and Research Station of Geohazards, China University of Geosciences, Wuhan 430074, China

creep tests. Zhou et al. (2020) analyzed the creep characteristics of soft rock under the coupling of stress and seepage through the creep test, and the crack evolution law was obtained. Zhu et al. (2022) studied the rheological characteristics of deep soft rock roadway by the true triaxial tests, and the evolution process of the rheological deformation of the roadway was revealed. On the other hand, considering the influence of different factors on the creep characteristics of soft rock, Ye et al. (2015) carried out triaxial creep tests on the soft rock at different temperatures, and the relation between creep failure time and minimum axial steady-state strain rate under different temperatures was obtained. Liu et al. (2018) carried out creep tests of soft rock under different relative humidity and clay mineral composition, and revealed the important influence of montmorillonite content on the creep deformation of clay rock, which provides an important reference and basis for the development of this study. In addition, many scholars have also conducted some tests from the perspective of engineering practice (Tan et al. 2019; Liu et al. 2021a, 2019; Ma et al. 2020).

The establishment of the rheological constitutive model provided a method effectively to solve the problem of the rheological failure mechanism of soft rock. For example, Arora and Gutierrez (2021) proposed a viscoelastic-plastic model to describe the creep characteristics of soft rock, and the Burgers model was modified. Ping et al. (2016) defined a new nonlinear damage creep constitutive model of high geo-stress soft rock by connecting the improved Burgers model and Hooke model in series. Tarifard et al. (2022) discussed the applicability of the Cvisc model in describing the creep process of soft rock. Shu et al. (2017) proposed a new nonlinear viscous coefficient Newton element, and established a nonlinear viscoelastic-plastic creep model of soft rock by connecting it with the Nishihara model in series. In addition, considering the influence of other factors on the creep constitutive equation, Xiong et al. (2017) established a unified constitutive model of advanced thermoelastic viscoelasticity of soft rock by introducing shear strength and over-consolidation evolution equation. Chen et al. (2022) established a Cvisc model considering the weakening coefficient of surrounding rock, and the fitting results showed that the model had good applicability to describe the whole creep process of soft rock. Wang et al. (2022) proposed a viscoelastic model based on the viscoelastic behavior of quartz and clay minerals, which provided some reference for the conduction of this study.

However, previous research did not consider the influence of mineral composition on the rheological properties of soft rock, and the rheological constitutive relation considering the physical characteristics of soft rock was rarely involved, which has a weak guiding role for the study of rheological properties of soft rock rich in clay minerals in western

mining regions. Therefore, in this study, taking the mudstone on the roof and floor in four typical mining regions as the research object, firstly, the clay mineral characteristic is analyzed by the X-ray diffraction test, and its rheological mechanical properties are obtained by the triaxial compression and creep tests. Further, based on the test results, the creep damage variable considering the characteristics of clay mineral is constructed, and the creep damage constitutive model of soft rock is established. Finally, the correctness of the creep damage constitutive model of soft rock is verified by fitting the test data.

2 Clay mineral characteristics of typical soft rock sample

2.1 Collection and preparation of samples

To obtain the characteristics of clay minerals of typical soft rock samples in the western regions and other regions, four types of soft rock samples were drilled for studying, including the roof mudstone of the No. 2 coal seam in Zaoquan Coal Mine of Ningmei Group (NY), the floor mudstone of No. 3-1 coal seam in Hongqingliang Coal Mine of Hao-hua Energy Group (HY), the roof mudstone of No. 8 coal seam in Luxi Coal Mine of Shandong Luneng Luxi Mining Co., Ltd. (LY), and Xinji No. 1 Coal Mine of China Coal Xinji Energy Co., Ltd (XY). The sites where the samples are drilled and some samples are shown in Fig. 1.

2.2 Analysis of clay mineral composition

The clay mineral characteristics of mudstone samples were analyzed by the X-ray diffraction (XRD) test. XRD is an important way to obtain information on mineral composition, atomic or molecular structure, and morphology of mineral crystals (Kuila et al. 2014). The Rigaku Ultima IV X-ray diffractometer was used in the test, as shown in Fig. 2, and the powder crystal method was used for testing. The sample for observation was manufactured by grinding and compacting, and the process is shown in Fig. 3. By the MDI Jade software, the X-ray diffraction pattern of mudstone samples is shown in Fig. 4.

Based on the test results, the main mineral types in different mudstone samples and the specific components of clay minerals are obtained. The specific analysis results are shown in Tables 1 and 2.

It can be seen from Table 1 that the main mineral components of mudstones in different regions include quartz, carbonate minerals, and clay minerals, among which the quartz and clay minerals account for the majority, which explains the typical argillaceous cementation



Fig. 1 The sites where the samples are drilled and some samples

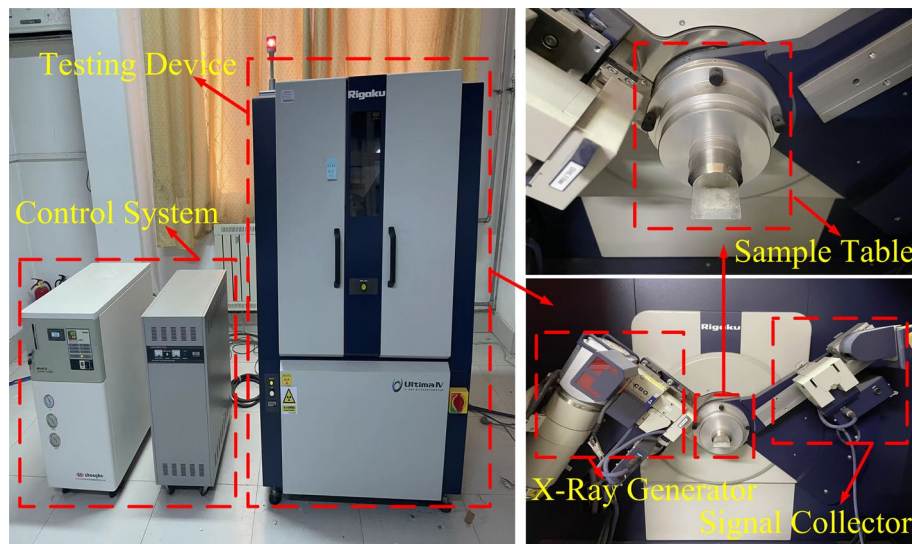


Fig. 2 X-ray diffractometer

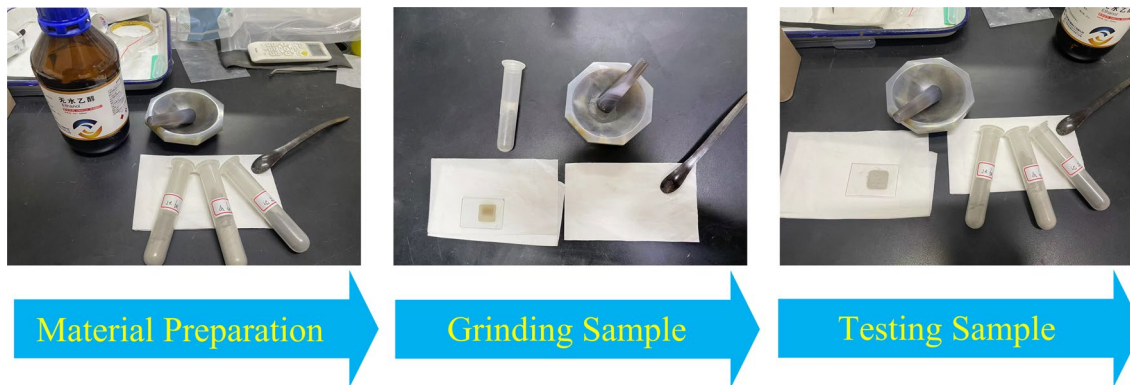


Fig. 3 Test process

characteristics of the mudstone. At the same time, the result shows that there are significant differences in the clay minerals content of mudstones in different regions. The clay minerals content in the northwestern regions

is obviously higher than that in the central and eastern regions. For example, the clay minerals content in NY and HY samples is 36.33% and 53.5%, and the LY and XY samples are 12.6% and 15.7%, respectively. In addition,

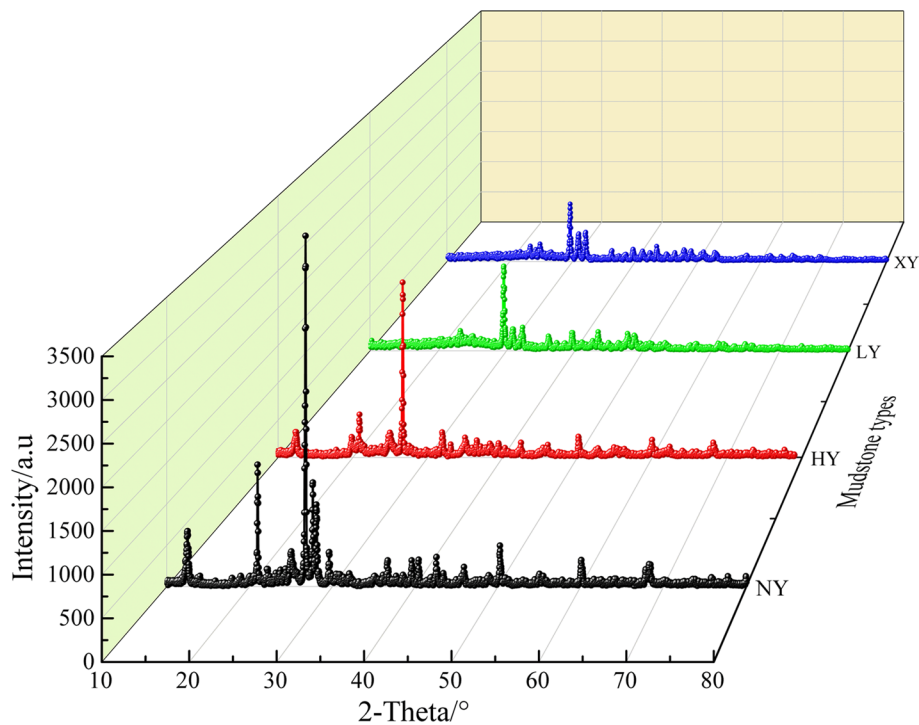


Fig. 4 X-ray diffraction pattern of typical mudstone samples

Table 1 Types and contents of minerals in typical mudstone samples

Sample	Types and contents of minerals (%)		
	Quartz	Carbonate mineral	Clay mineral
NY	50.92	12.75	36.33
HY	29.75	16.75	53.50
LY	80.66	6.74	12.60
XY	51.60	32.70	15.70

Table 2 The specific composition and content of clay minerals

Sample	Relative content of clay mineral composition (%)			
	Kaolinite	Montmorillonite	Illite	Illite-montmorillonite mixed layer
NY	46.24	11.19	13.12	29.45
HY	65.78	8.24	4.32	21.66
LY	70.98	3.96	5.79	19.27
XY	68.28	3.56	10.98	17.18

it can be found from Table 2 that the content of kaolin in mudstone accounts for about 45% to 75%, the illite-montmorillonite mixed layer accounts for about 17% to 30%, and the montmorillonite ranges from 3% to 12%.

3 Rheological properties of soft rock with different clay mineral contents

3.1 Triaxial compression test under different confining pressures

The load in triaxial creep test is of great significance for ensuring the accuracy and reliability of the creep test results, which is generally determined by the triaxial compression test under different confining pressures. Due to the limitation of the content of the paper, the process of triaxial compression test is not described here, and the test results are shown in Table 3.

Combined with Tables 2 and 3, there is a clear relation between the content of montmorillonite and illite-montmorillonite mixed layer in clay minerals and the mechanical properties of mudstone samples. With the increase of the content of montmorillonite and illite-montmorillonite mixed layer, the triaxial compression strength, internal friction angle, and cohesion of mudstone under the same confining pressure show a significant decreasing trend, and Poisson's ratio shows an increasing trend. As shown in Fig. 5, when the confining pressure is 2 MPa, the triaxial compressive strength of NY sample is decreased by 48.99% compared with XY sample, the internal friction angle and cohesion is

Table 3 Main mechanical parameters of typical mudstone

Sample	Confining pressure (MPa)	Compressive strength (MPa)	Poisson's ratio	Internal friction angle (°)	Cohesion (MPa)
NY	2	17.63	0.285	37.77	2.9
	4	25.43	0.271		
	6	30.96	0.259		
	8	36.78	0.243		
HY	2	19.67	0.254	39.15	3.2
	4	27.62	0.232		
	6	34.12	0.201		
	8	41.29	0.192		
LY	2	25.87	0.238	42.68	3.7
	4	33.12	0.209		
	6	42.56	0.184		
	8	50.67	0.179		
XY	2	34.56	0.232	46.34	4.9
	4	45.14	0.176		
	6	56.32	0.142		
	8	65.69	0.124		

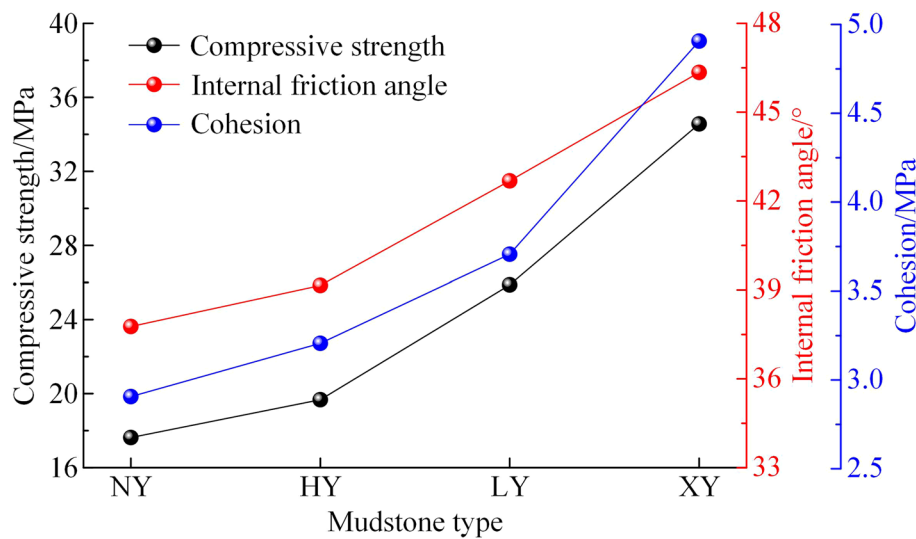


Fig. 5 Variation characteristics of mechanical properties of mudstone samples

decreased by 18.49% and 40.82%, respectively. It could be seen that the increase of the content of montmorillonite and illite-montmorillonite mixed layer has a significant weakening effect on the triaxial compressive strength, internal friction angle, and cohesion of mudstone.

3.2 Scheme of triaxial creep test

To obtain the rheological mechanical characteristics of mudstone under different clay mineral contents, especially the

influence of different montmorillonite and illite-montmorillonite mixed layer contents on the rheological mechanical characteristics of mudstone, the creep test of the mudstone samples under different confining pressures was carried out by the RLJW-2000 rock servo pressure test machine (Fig. 6). The loading speed of the test machine is 0.05–0.5 mm/min, the maximum axial force is 2000 kN, and the maximum confining pressure is 50 MPa, which can satisfy the test requirements.

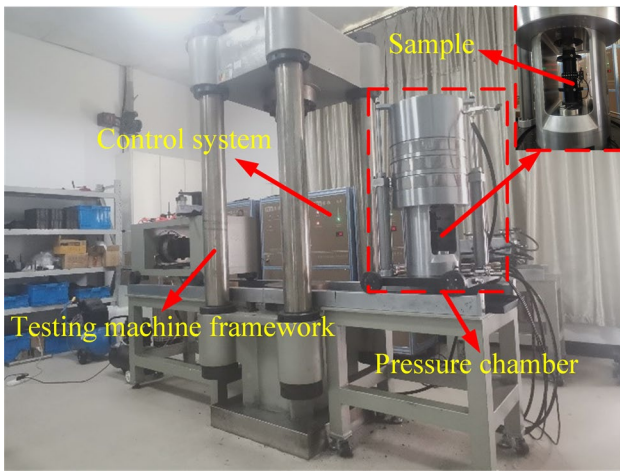


Fig. 6 RLJW-2000 rock servo pressure test machine

During the creep tests, the first-stage load is applied to the sample, which the value is equal to 30% of the compression strength, and then it is increased by 5% of the compression strength in each stage until the sample is destroyed. The loading rate is 0.1 MPa/min, and the creep time of each stage is 4 h.

3.3 Analysis of creep test results

3.3.1 Characteristics of creep deformation

Creep deformation is an important index to analyze the long-term stability of surrounding rock in underground engineering. According to the loading scheme, the creep test was carried out for mudstone samples. The results are shown in Fig. 7.

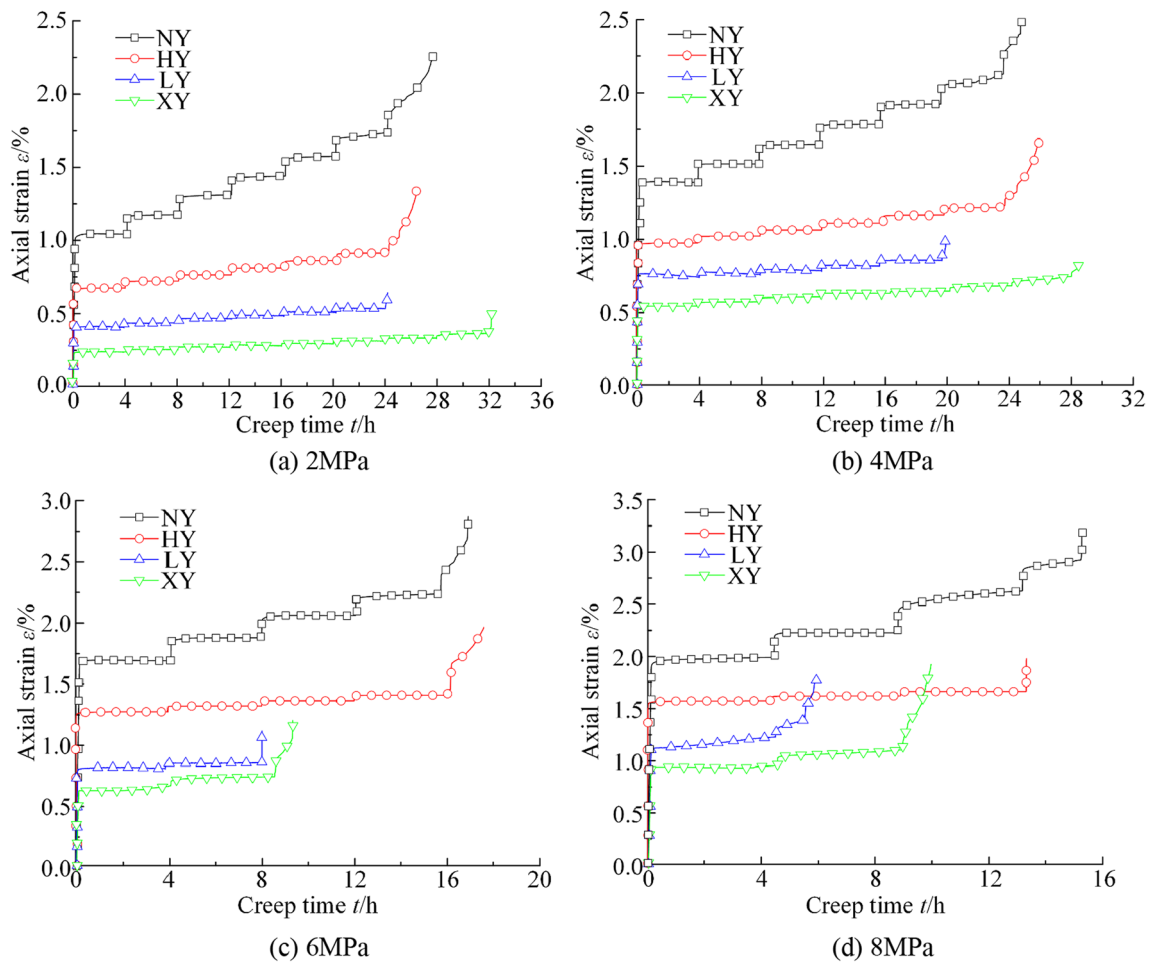


Fig. 7 Creep test results

By comparing the creep deformation of mudstone samples under the same loading stage, it can be found that the axial load of NY sample is the smallest, but its creep deformation is the largest under the same confining pressure. As for the initial creep deformation, for example, when the confining pressure is 2 MPa, the deformation of NY sample is 1.02%, which is about 3.25 times larger than XY sample. However, the axial load of NY sample is 50.96% of XY. The result shows that the creep deformation of mudstone is not only related to the load, but also related to its properties. Combined with the above analysis of clay mineral composition, the creep deformation of mudstone has a good correlation with the content of montmorillonite and illite-montmorillonite mixed layer. In other words, the creep deformation of soft rock increases significantly with the increase of montmorillonite and illite-montmorillonite mixed layer content.

When the axial load increases gradually, the sample will eventually enter the accelerated-speed creep stage, but the timing of entering the accelerated-speed creep is different due to the different montmorillonite and illite-montmorillonite mixed layer content. For example, when the confining pressure is 2 MPa, the axial load of the NY sample is 10.6 MPa when it occurs accelerated-speed creep, but the XY sample is 24.2 MPa. It can be seen that the increase in the content of montmorillonite and illite-montmorillonite mixed layer will significantly decrease the strength of mudstone, resulting in occurring accelerated-speed creep under low stress.

In summary, the creep deformation of mudstone samples is not only related to the deviatoric stress, but also to the content of montmorillonite and illite-montmorillonite mixed layer. In other words, with the increase of montmorillonite

and illite-montmorillonite mixed layer content, the creep deformation of mudstone shows an obvious increasing trend, and the time to enter accelerated-speed creep is advanced.

3.3.2 Characteristics of the viscosity coefficient

The viscosity coefficient is a characteristic index of creep and flow of soft rock, which reflects the rheological properties of materials, and the value can be obtained according to the slope of the stress–strain rate curve. For example, when the confining pressure is 2 MPa, the relation between the viscosity coefficient of mudstone and the creep time under different montmorillonite and illite-montmorillonite mixed layer content is shown in Fig. 8.

Figure 8 shows that the viscosity coefficient with different montmorillonite and illite-montmorillonite mixed layer content is significantly different, which increases in the form of power function with the decrease of montmorillonite and illite-montmorillonite mixed layer content. For example, the viscosity coefficient of XY sample is 2.54×10^9 MPa s, and the NY sample is 4.93×10^8 MPa s, which is decreased by 80.59% compared with XY sample. It can be seen that the increase of montmorillonite and illite-montmorillonite mixed layer content has a significant weakening effect on the viscosity coefficient of mudstone.

3.3.3 Characteristics of long-term strength

Long-term strength is an important parameter to distinguish stable creep and unstable creep stages, and it is also an important reference for evaluating the long-term stability of underground engineering. The traditional methods to determine the long-term strength include the transitional creep method and the isochronal curve method (Salmi et al. 2020; Hamza and Stace 2018; Atsushi and Hani 2017). Transitional creep method can only determine a certain range for long-term strength, but cannot obtain the specific values, which is of little guiding significance to the engineering. Although the isochronal curve method is relatively simple, it requires a large number of test data under different conditions to fit and analyze it. The process is extremely complicated, which easily leads to the accumulation of test error, resulting in inaccurate calculation results.

Some scholars obtained the long-term strength by the inflection point of the relation between stable creep rate and stress. Wang et al. (2018) proposed an improved inflection point method of stable creep rate and discussed its feasibility, which indicated the intersection of the two curves obtained by fitting the reciprocal of stable creep

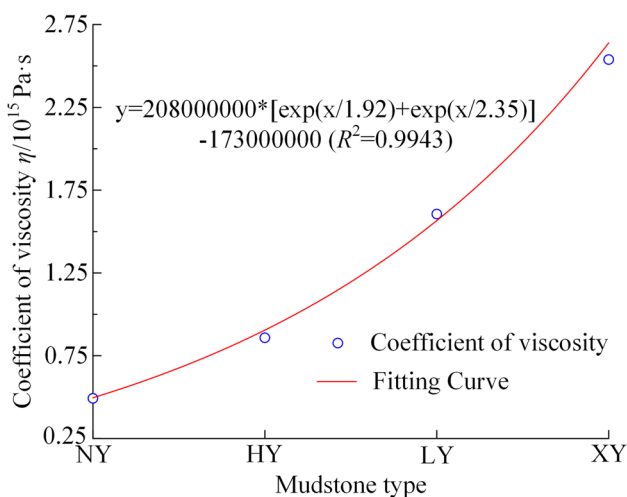


Fig. 8 Curve of the viscosity coefficient

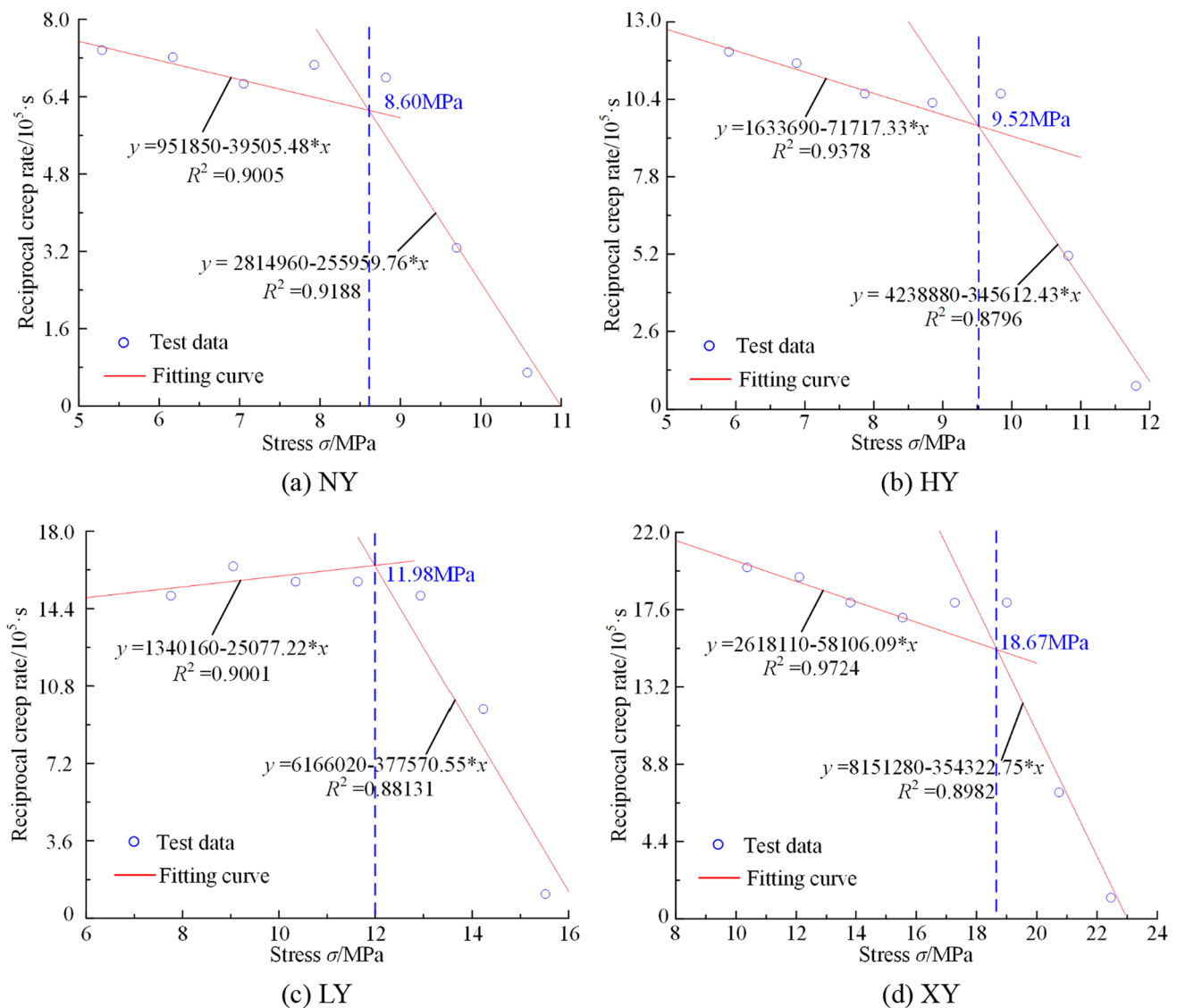


Fig. 9 Determination of long-term strength of mudstone

rate and low/high stress is the long-term strength of rock. In this study, the long-term strength of mudstone with different montmorillonite and illite-montmorillonite mixed layer content is obtained by using this method. Taking the confining pressure of 2 MPa as an example, as shown in Fig. 9.

For the mudstone samples of NY, HY, LY, and XY, the long-term strength obtained by the above method is 8.60, 9.52, 11.98, and 18.67 MPa, respectively, and the NY sample is decreased by about 53.94% compared with the XY sample. It can be seen that the long-term strength decreases with the increase of montmorillonite and illite-montmorillonite mixed layer content, which is consistent with the above creep test results. That is, the integrity of mudstone is decreased by the increase of montmorillonite

and illite-montmorillonite mixed layer content, which ultimately leads to the decrease of stress conditions for occurring accelerated-speed creep of mudstone.

4 M-S creep damage constitutive model of soft rock

In order to further explain the creep failure mechanism of soft rock with different clay mineral content, combined with the above test results, the creep damage variables of soft rock can be put forward, and the creep damage constitutive model can be constructed, which can provide an important method and idea for this study.

4.1 Relation between montmorillonite content and mechanical parameters

Based on the above test results, the strength and internal friction angle of soft rock will obviously decrease with the increase of montmorillonite and illite-montmorillonite mixed layer content. At the same time, for the shear strength of clay minerals, many studies have shown that kaolinite is the largest, followed by illite, and montmorillonite is the lowest, which explains that the content of montmorillonite has a significantly weakening effect on the strength of clay minerals (Kang 1993). Therefore, the relation between montmorillonite content and internal friction angle can be established by combining the XRD and triaxial compression test results. Considering the number of samples, the internal friction angle of soft rock under different montmorillonite content was investigated combined with the existing research about the physical composition analysis of mudstone samples and its mechanical properties (Liu 2022; Zhou 2022; Wang 2022; Jin 2021), as shown in Table 4. Kang (1993) discussed the relation between mineral composition and mechanical properties of soft rock, and the fitting function adopted in this study is based on that, as shown in Fig. 10.

As shown in Table 4, The BY sample is the Purple red mudstone of T₂b² member of typical Badong Formation in western Hubei-eastern Chongqing area, the FY sample is the landslide mudstone in Xiangning, Linfen, the JY sample is the landslide mudstone in Zezhou, Jincheng, the MY sample is the floor mudstone of 3⁻¹ coal seam in Anshan Coal Mine of Miaohagu mining area, the SY sample is the roof mudstone of the No. 2 coal seam in Shanghaimiao mining area, the TY sample is the landslide mudstone in Dongshan, Taiyuan, and the VY sample is the landslide mudstone in Linxian, Lvliang.

Table 4 Relation between montmorillonite content and internal friction angle of mudstone in different regions (Liu 2022; Zhou 2022; Wang 2022; Jin 2021)

Sample	Relative content of montmorillonite in clay minerals (%)	Internal friction angle (°)
BY	2.80	45.55
FY	32.76	17.74
HY	8.24	39.15
JY	17.74	22.78
LY	3.96	42.68
MY	39.62	17.60
NY	11.19	37.77
SY	28.00	22.95
TY	13.11	25.17
VY	29.79	21.31
XY	3.56	46.34

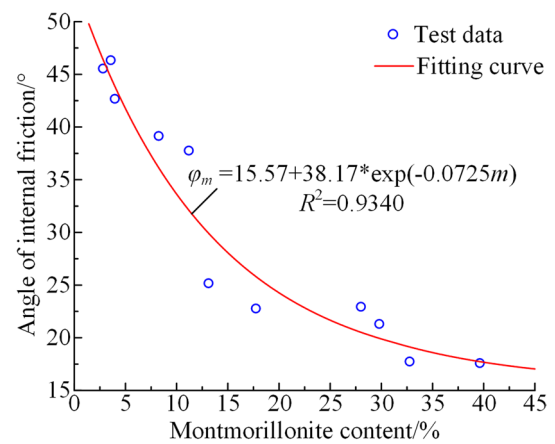


Fig. 10 Fitting result

The relation between the internal friction angle and montmorillonite can be obtained:

$$\varphi_m = 15.57 + 38.17 \exp(-0.0725m) \tag{1}$$

where, φ_m is the internal friction angle of soft rock under different montmorillonite content, °; m is the montmorillonite content, %.

According to the Mohr–Coulomb strength theory and the envelope theorem of the Mohr circle, the general calculation equation between cohesion c and internal friction angle φ can be obtained (Yang et al. 2007).

$$c = \frac{\sigma_c}{2\sqrt{K}}$$

$$\varphi = \tan\left(\frac{K-1}{2\sqrt{K}}\right) \tag{2}$$

where, K is related to the rock material itself; σ_c is the uniaxial compressive strength, MPa.

Based on Eqs. (1) and (2), the expression of cohesion c_m with different montmorillonite content can be obtained:

$$c_m = \frac{\sigma_c}{2\sqrt{1 + 2tg^2\varphi_m(1 \pm 1/\sin\varphi_m)}} \tag{3}$$

4.2 Construction of creep damage model

4.2.1 Definition of damage variable

Damage has always been an important research direction in creep constitutive relation, especially the definition of damage variable and the solution of damage evolution equation. As early as 1971, Lemaitre et al. (1971) proposed

the equivalent strain hypothesis. Based on this method, the stress without damage is changed into effective stress, and the damage constitutive equation can be established:

$$\epsilon_e^* = \frac{\sigma}{E} = \frac{\sigma^*}{(1-D)E_0} \tag{4}$$

where, ϵ_e^* is the equivalent elastic strain; σ^* is the effective stress; MPa, D is the damage variable; E_0 is the elastic modulus of soft rock without damage, GPa.

The damage variable D can be expressed as:

$$D = 1 - \frac{E_t}{E_0} \tag{5}$$

Duncan-Chang model is established based on a large number of triaxial test results, which describes the hyperbolic relation between deviatoric stress and axial strain (Zhang et al. 2018), as shown in Eq. (6). The related work of this study is carried out on its basis.

$$\sigma_1 - \sigma_3 = \frac{\epsilon_1}{a + b\epsilon_1} \tag{6}$$

where ϵ_1 is the axial strain.

During the process of triaxial compression, there is a certain relation between axial strain and time, so the above equation can be expressed as:

$$\sigma_1 - \sigma_3 = \frac{t}{a + bt} \tag{7}$$

where a and b are related to the rock material itself.

During the loading process of the sample, based on Eq. (7), the elastic modulus E_t at any time has the following relation:

$$\frac{d(\sigma_1 - \sigma_3)}{dt} = E_t = \frac{a + 2bt}{(a + bt)^2} \tag{8}$$

When the sample is initially loaded, ϵ is 0, there is

$$\frac{1}{a} = E_0 \tag{9}$$

When the sample reaches the compression strength during the triaxial loading process:

$$\sigma_1 - \sigma_3 = \frac{2c \cos \varphi + 2\sigma_3 \sin \varphi}{1 - \sin \varphi} \tag{10}$$

Combined with Eqs. (6) and (10):

$$\frac{2c \cos \varphi + 2\sigma_3 \sin \varphi}{1 - \sin \varphi} = \frac{\epsilon_{\max}}{a + b\epsilon_{\max}} \tag{11}$$

where ϵ_{\max} is the corresponding strain when the rock reaches the compression strength.

Combined with Eqs. (9) and (11):

$$b = \frac{(1 - \sin \varphi)E_0\epsilon_{\max} - 2(c \cos \varphi + \sigma_3 \sin \varphi)}{2E_0\epsilon_{\max}(c \cos \varphi + \sigma_3 \sin \varphi)} \tag{12}$$

The relation between parameter b and montmorillonite content m in Duncan-Chang model can be obtained by combining with the Eqs. (2), (3), and (12):

$$b = \frac{(1 - \sin \varphi_m)E_0\epsilon_{\max} - 2(c_m \cos \varphi_m + \sigma_3 \sin \varphi_m)}{2E_0\epsilon_{\max}(c_m \cos \varphi_m + \sigma_3 \sin \varphi_m)} \tag{13}$$

At the same time, the Eq. (7) is further simplified:

$$E_t = \frac{1}{a} \left(1 - \frac{1}{\left(1 + \frac{a}{bt}\right)^2} \right) \tag{14}$$

Therefore,

$$E_t = E_0 \left(1 - \frac{1}{\left(1 + \frac{1}{bE_0t}\right)^2} \right) \tag{15}$$

Based on the Eq. (5), the damage variable can be expressed at:

$$D = 1 - \frac{E_t}{E_0} = 1 - \left(1 - \frac{1}{\left(1 + \frac{1}{bE_0t}\right)^2} \right) \tag{16}$$

It can be seen that the damage variable D increases with the increase of time, ranging from 0 to 1, which conforms to the evolution law of damage variables and has high reliability.

Thus, the damage constitutive equation can be established:

$$\sigma = \left(1 - \frac{1}{\left(1 + \frac{1}{bE_0t}\right)^2} \right) E_0 \epsilon \tag{17}$$

where

$$b = f(m, \sigma_3) = \frac{(1 - \sin \varphi_m)E_0\epsilon_{\max} - 2(c_m \cos \varphi_m + \sigma_3 \sin \varphi_m)}{2E_0\epsilon_{\max}(c_m \cos \varphi_m + \sigma_3 \sin \varphi_m)} \tag{18}$$

According to Eq. (17), the damage of soft rock during triaxial loading can be divided into two aspects: On the one hand, the damage of soft rock is greatly affected by its montmorillonite content and confining pressure in the initial loading stage. The damage at this time can be defined as the initial damage. On the other hand, during the middle and late stage of loading, the damage is mainly affected by material strain, and the damage at this time can be defined as

Fig. 11 Cvisc rheological constitutive model

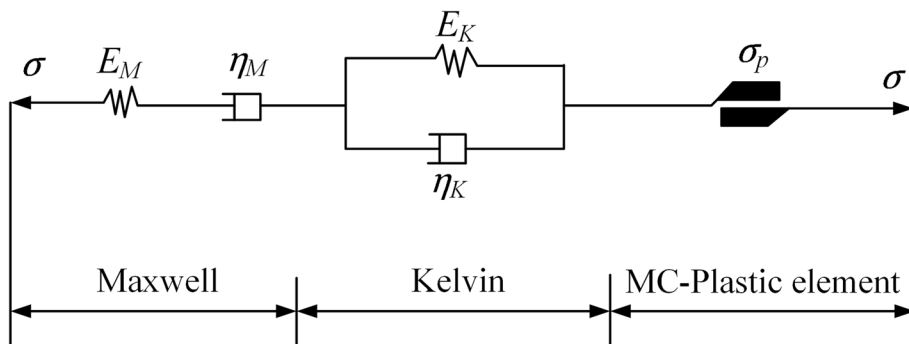
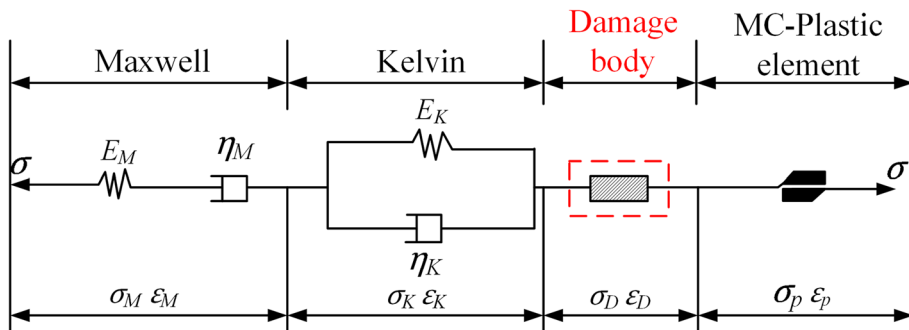


Fig. 12 M–S creep damage constitutive model of soft rock



the loading damage. The initial damage and loading damage together constitute the nature of the damage of soft rock with montmorillonite.

4.2.2 M–S creep damage model

Cvisc model is a composite viscoelastic-plastic model composed of the Burgers model and the Mohr–Coulomb model in series, which has good applicability to describe the creep behavior of soft rock dominated by shear failure. Especially for the damage constitutive equation established in this study, the shear strength indexes such as cohesion and internal friction angle are comprehensively considered, so the Cvisc model can better explain the influence of the damage variable. In the one-dimensional stress state, the Cvisc model is shown in Fig. 11.

Considering the influence of initial damage and loading damage, the M–S (Montmorillonite–Stress) soft rock creep damage constitutive model is established by connecting the damaged body and the Cvisc model, as shown in Fig. 12.

When the two ends of the model are subjected to external stress, the strain generated by the whole model is the sum of the strains generated by each part, and the stress of the whole model is equal to that of each part, that is:

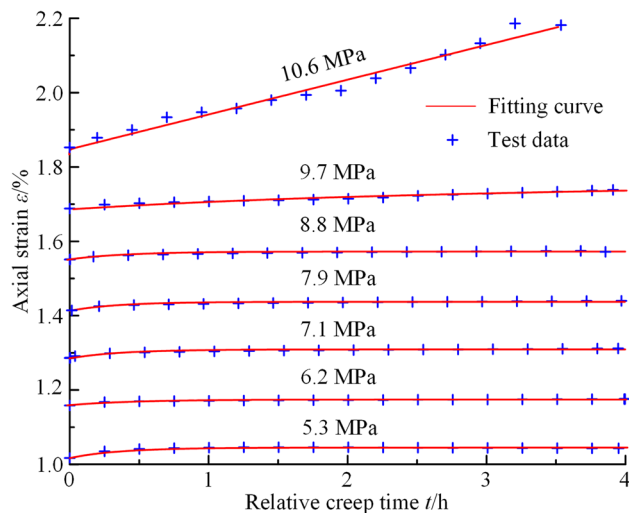


Fig. 13 Fitting results of NY sample (confining pressure 2 MPa)

$$\begin{cases} \sigma = \sigma_M + \sigma_K + \sigma_D + \sigma_p \\ \varepsilon = \varepsilon_M + \varepsilon_K + \varepsilon_D + \varepsilon_p \end{cases} \quad (19)$$

where σ_M , σ_K , σ_D , and σ_p are the stress of Maxwell’s body, Kelvin’s body, Damage body, and the yield stress of

Table 5 Fitting constants and determination coefficients

Axial stress	E_M (MPa)	η_M (GPa s)	E_K (MPa)	η_K (GPa s)	a	b	R^2
5.3	7.468	1.000e+11	251.6	0.090	5.966×10^{-8}	2.198×10^{-8}	0.9283
6.2	6.271	1.000e+11	351.6	0.162			0.9046
7.1	5.440	1.000e+11	251.6	0.090			0.9070
7.9	4.807	1.000e+11	251.6	0.090			0.9602
8.8	4.281	1.000e+11	251.6	0.100			0.9020
9.7	3.861	1.100	160	0.251			0.9501
10.6	3.456	0.053	10,010	0.010			0.9741

MC-Plastic elements, respectively, ε_M , ε_K and ε_D are the strain of Maxwell's body, Kelvin's body, and Damage body, respectively, ε_p is the corresponding strain under the yield stress.

Combined with the Cvisc creep model, the M–S creep damage model can be expressed:

$$\left\{ \begin{array}{l} \varepsilon(t) = \frac{\sigma_0}{E_M} + \frac{\sigma_0}{\eta_M} t + \frac{\sigma_0}{E_K} \left[1 - \exp\left(-\frac{E_K}{\eta_K} t\right) \right] + \frac{\sigma_0}{\left(1 - \frac{1}{\left(1 + \frac{a}{br}\right)^2}\right)^{\frac{1}{a}}}, \sigma < \sigma_p \\ \varepsilon(t) = \frac{\sigma_0}{E_M} + \frac{\sigma_0}{\eta_M} t + \frac{\sigma_0}{E_K} \left[1 - \exp\left(-\frac{E_K}{\eta_K} t\right) \right] + \frac{\sigma_0}{\left(1 - \frac{1}{\left(1 + \frac{a}{br}\right)^2}\right)^{\frac{1}{a}}} + \varepsilon_p, \sigma \geq \sigma_p \end{array} \right. \quad (20)$$

where E_M and E_K are the elastic modulus of Maxwell's body and Kelvin's body, GPa, η_M , and η_K are the viscosity coefficient of Maxwell body and Kelvin body, Pa s, which can be obtained by fitting the test data, t is the creep time, s.

4.3 Verification of constitutive model

In order to verify the correctness of the M–S creep damage constitutive model proposed in this paper, Eq. (17) is used to fit the creep test result of NY sample under confining pressure of 2 MPa. The fitting tool adopts the Curve Fitting Toolbox in MATLAB, and the fitting algorithm is the Trust-Region-Reflective Algorithm. The fitting results are as shown in Fig. 13, and the fitting constants are shown in Table 5.

Figure 13 shows that the calculated results of the model are consistent with the creep test result. The determination coefficients are 0.9020–0.9741, which indicates that the M–S creep damage constitutive model of soft rock proposed in this paper has good practicability and reliability.

5 Discussion

Currently, some scholars have obtained the damage failure mechanism of soft rock by various methods (Xie et al. 2019; Liu et al. 2021b; Li et al. 2022; Torabi-Kaveh et al. 2022). However, the creep damage mechanism and long-

term stability of soft rock are not only affected by stress, but also by its physical characteristics. Especially for the western mining regions where are rich in clay minerals in coal-bearing strata, this effect is more obvious (Sun et al. 2021; Fan et al. 2022; Jin et al. 2023; Guo et al. 2019). Many scholars have carried out a lot of creep tests on soft rock to obtain the creep characteristics, such as the step-loading tests, stress-seepage coupling creep test, and creep test under the influence of different temperatures, relative humidity, and other factors (Chen et al. 2021; Zhou et al. 2020; Liu et al. 2020). The research results provide a reference for revealing the creep characteristics of soft rock.

Compared with previous studies, the main focus of this study is to establish the relation between the composition and content of clay minerals in soft rock and their creep characteristics. Therefore, taking the mudstone samples in four typical mining regions, the similarities and differences of creep mechanical properties are analyzed and revealed based on the differences in clay mineral composition and content. The results show that the content of clay minerals in the northwestern regions is higher than that in the central

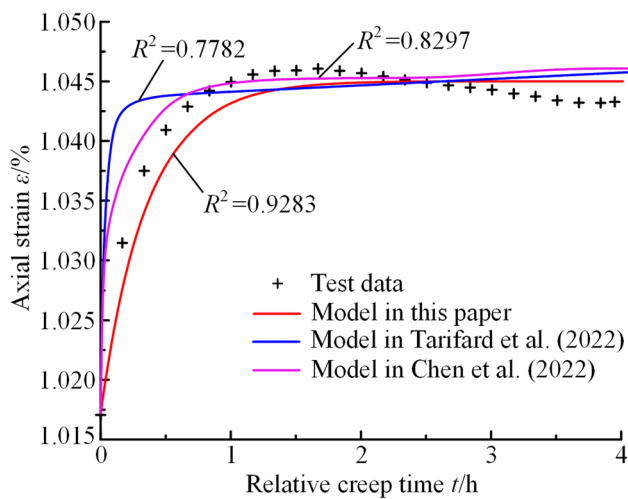


Fig. 14 Comparison of fitting results

and eastern regions, and the rheological properties of mudstones in different regions are also different, which is consistent with the existing research (Sun et al. 2021; Chen et al. 2021). In addition, the difference of clay minerals content such as montmorillonite and illite-montmorillonite mixed layer in mudstone samples have a good correlation with their rheological properties. The higher the content of clay minerals, the greater the creep deformation of soft rock, the earlier the soft rock enters the accelerated-speed creep, the greater the creep deformation rate, the smaller the viscosity coefficient, and the lower the long-term strength. This research results have not been found in previous studies, which can provide a more accurate reference for the design and construction of underground engineering in western mining regions.

The rheological constitutive model is one of the research hotspots in recent years, which provides an effective method to reveal the creep damage mechanism of soft rock. However, most of the existing constitutive models mostly consider the influence of external factors, the influence of mineral composition on the rheological properties of soft rock is rarely involved, and the rheological constitutive relation considering the physical characteristics of soft rock has not yet been established. When they are used to study the mechanical properties of soft rock with the same lithology but different clay mineral content, the error is unacceptable. For example, when the creep model of soft rock established by Tarifard et al. (2022) and Chen et al. (2022) is used to fit the creep test results of NY sample under confining pressure of 2 MPa (Axial load is 5.3 MPa), as shown in Fig. 14, and the determination coefficients are only 0.7782 and 0.8297, respectively. However, the M–S creep damage constitutive model of soft rock established in this study has high fitting accuracy to the test results, and the determination coefficient

can reach 0.9283. The model established in this study comprehensively reflects the influence of clay mineral content and stress level of soft rock, which provides an innovative method for revealing the creep deformation mechanism of soft rock rich in clay minerals in the western mining regions and carrying out the study on the stability control of soft rock roadway.

In summary, compared with previous studies, the rheological mechanical properties of soft rock with different clay mineral contents are accurately obtained in this study, and the M–S creep damage constitutive model considering the difference in clay mineral content is established. The research results have important scientific value for correctly understanding the influence of clay minerals on the rheological properties of soft rock and revealing the relation between clay mineral content and creep damage mechanism. At the same time, it also provides a more accurate method for studying the failure mechanism of soft rock roadway rich in clay minerals in western mining regions. In future research, it is necessary to discuss the influence of other physical components on the rheological mechanical properties and establish the corresponding constitutive model for revealing deeply the creep damage mechanism of soft rock.

6 Conclusions

- (1) With the increase of clay mineral content such as montmorillonite and illite-montmorillonite mixed layer, the mechanical properties of mudstone under the same confining pressure show a significant decrease trend. For example, compared with XY sample, the triaxial compressive strength, internal friction angle and cohesion of NY sample decreases by about 48.99%, 18.49% and 40.82%, respectively.
- (2) With the increase of clay mineral content and stress level, the creep deformation of mudstone shows a significant increasing trend, while the viscosity coefficient and long-term strength show a decreasing trend. For example, compared with the XY sample, the initial creep deformation of the NY sample is increased by 3.25 times, the viscosity coefficient and long-term strength are decreased by 80.59% and 53.94%, respectively.
- (3) A creep damage variable considering the initial damage and loading damage is constructed, and the M–S creep damage constitutive model of soft rock is established. The new creep damage model can comprehensively reflect the influence of physical composition, damage and viscous characteristics on the rheological mechanical properties, which provides an important method for studying the failure mechanism of soft rock roadway rich in clay minerals in western mining regions.

Acknowledgements This study was supported by the National Natural Science Foundation of China (52174122, 52074168); Excellent Youth Fund of Shandong Natural Science Foundation (ZR2022YQ49); Climbing Project of Taishan Scholar in Shandong Province (tspd20210313); and Young Expert of Taishan Scholar Project in Shandong Province (tsqn202211150).

Declarations

Competing interests The authors declare that they have no competing interests.

Open Access This article is licensed under a Creative Commons Attribution 4.0 International License, which permits use, sharing, adaptation, distribution and reproduction in any medium or format, as long as you give appropriate credit to the original author(s) and the source, provide a link to the Creative Commons licence, and indicate if changes were made. The images or other third party material in this article are included in the article's Creative Commons licence, unless indicated otherwise in a credit line to the material. If material is not included in the article's Creative Commons licence and your intended use is not permitted by statutory regulation or exceeds the permitted use, you will need to obtain permission directly from the copyright holder. To view a copy of this licence, visit <http://creativecommons.org/licenses/by/4.0/>.

References

- Arora K, Gutierrez M (2021) Viscous-elastic-plastic response of tunnels in squeezing ground conditions: analytical modeling and experimental validation. *Int J Rock Mech Min* 146:104888. <https://doi.org/10.1016/j.ijrmms.2021.104888>
- Atsushi S, Hani SM (2017) Numerical investigation into pillar failure induced by time-dependent skin degradation. *Int J Rock Mech Min* 27(4):591–597. <https://doi.org/10.1016/j.ijmst.2017.05.002>
- Chen XY, Wang XF, Zhang DS, Qin DD, Wang Y, Wang JY, Chang ZC (2021) Creep and control of the deep soft rock roadway (DSRR): insights from laboratory testing and practice in Pingdingshan mining area. *Rock Mech Rock Eng* 55(1):363–378. <https://doi.org/10.1007/S00603-021-02670-1>
- Chen FB, Su R, Yang LH, Yang XL, Jiao HZ, Zhu CX (2022) Study on surrounding rock deformation laws of an argillaceous soft rock roadway based on the creep damage model. *Front Earth Sci* 10:914170. <https://doi.org/10.3389/feart.2022.914170>
- Fan DY, Liu XS, Tan YL, Li XB, Lkhamsuren P (2022) Instability energy mechanism of super-large section crossing chambers in deep coal mines. *Int J Min Sci Technol* 32(5):1075–1086. <https://doi.org/10.1016/j.ijmst.2022.06.008>
- Guo ZB, Wang Q, Yin SY, Kuai XH, Yan DS, Li MY, Qu YD (2019) The creep compaction behavior of crushed mudstones under the step loading in underground mining. *Int J Coal Sci Technol* 6(3):408–418. <https://doi.org/10.1007/s40789-019-0243-8>
- Hamza O, Stace R (2018) Creep properties of intact and fractured muddy siltstone. *Int J Rock Mech Min* 106:109–116. <https://doi.org/10.1016/j.ijrmms.2018.03.006>
- Jin YQ (2021) Study on formation mechanism of landslide controlled by soft rock in coal measure strata of Shanxi Province. Thesis, Taiyuan University of Technology
- Jin YF, Zhang AJ, Yin ZY, Zhu QY, Wang JH (2013) One-dimensional compressibility of soft clay related to clay minerals. *Chin J Geotech Eng* 35(1):131–136
- Jin YX, Geng J, Lv C, Chi Y, Zhao TD (2023) A methodology for equipment condition simulation and maintenance threshold optimization oriented to the influence of multiple events. *Reliab Eng Syst Saf* 229:108879. <https://doi.org/10.1016/j.res.2022.108879>
- Kang HP (1993) Mechanism and prevention of floor heave in soft rock roadway. China Coal Industry Publishing House, Beijing
- Kuila U, McCarty DK, Derkowski A, Fischer TB, Topor T, Prasad M (2014) Nano-scale texture and porosity of organic matter and clay minerals in organic-rich mudrocks. *Fuel* 135:359–373. <https://doi.org/10.1016/j.fuel.2014.06.036>
- Lemaitre J (1971) Evaluation of dissipation and damage in metals submitted to dynamic loading. In: Proceedings of international conference on mechanical behavior of materials Kyoto, Japan: The Society of Material Science
- Li XB, Liu XS, Tan YL, Ma Q, Wu BY, Wang HL (2022) Creep constitutive model and numerical realization of coal-rock combination deteriorated by immersion. *Minerals* 12(3):292. <https://doi.org/10.3390/min12030292>
- Liu WL (2022) Study on engineering geological characteristics and pregnant sliding mechanism of Badong Formation slope with mudstone interlayer. Dissertation, China University of Geosciences
- Liu ZB, Shao JF, Xie SY, Conil N, Zha WH (2018) Effects of relative humidity and mineral compositions on creep deformation and failure of a claystone under compression. *Int J Rock Mech Min* 103:68–76. <https://doi.org/10.1016/j.ijrmms.2018.01.015>
- Liu XL, Wang F, Huang J, Wang SJ, Zhang ZZ, Nawit K (2019) Grout diffusion in silty fine sand stratum with high groundwater level for tunnel construction. *Tunn Undergr Space Technol* 93:103051. <https://doi.org/10.1016/j.tust.2019.103051>
- Liu KQ, Rassouli FS, Liu B, Ostadhassan M (2020) Creep behavior of shale: nanoindentation vs. triaxial creep tests. *Rock Mech Rock Eng* 54(1):321–335. <https://doi.org/10.1007/s00603-020-02255-4>
- Liu XS, Fan DY, Tan YL, Ning JG, Song SL, Wang HL, Li XB (2021a) New detecting method on the connecting fractured zone above the coal face and a case study. *Rock Mech Rock Eng* 54:4379–4391. <https://doi.org/10.1007/s00603-021-02487-y>
- Liu XS, Song SL, Tan YL, Fan DY, Ning JG, Li XB, Yin YC (2021b) Similar simulation study on the deformation and failure of surrounding rock of a large section chamber group under dynamic loading. *Int J Min Sci Technol* 31(3):495–505. <https://doi.org/10.1016/j.ijmst.2021.03.009>
- Ma Q, Tan YL, Liu XS, Gu QH, Li XB (2020) Effect of coal thicknesses on energy evolution characteristics of roof rock-coal-floor rock sandwich composite structure and its damage constitutive model. *Compos Part B Eng* 198:108086. <https://doi.org/10.1016/j.compositesb.2020.108086>
- Montero-Cubillo NS, Galindo RA, Olalla C, Muniz-Menendez M (2021) Pull-out creep laboratory test for soft rocks. *Int J Rock Mech Min* 144:104811. <https://doi.org/10.1016/j.ijrmms.2021.104811>
- Ping C, Wen YD, Wang YX, Yuan HP, Yuan BX (2016) Study on nonlinear damage creep constitutive model for high-stress soft rock. *Environ Earth Sci* 75(10):900. <https://doi.org/10.1007/s12665-016-5699-x>
- Salmi EF, Malinowska A, Hejmanowski R (2020) Investigating the post-mining subsidence and the long-term stability of old mining excavations: case of Cow Pasture Limestone Mine, West Midlands, UK. *Bull Eng Geol Environ* 79(1):225–242. <https://doi.org/10.1007/s10064-019-01575-2>
- Shu ZL, Liu BX, Huang S, Wei YH, Zhao BY (2017) Nonlinear viscoelasto-plastic creep model of soft rock and its parameters identification. *J Min Saf Eng* 34(4):803–809. <https://doi.org/10.13545/j.cnki.jmse.2017.04.028>
- Sun LH, Ji HG, Yang BS (2019) Physical and mechanical characteristic of rocks with weakly cemented strata in Western

- representative mining area. *J China Coal Soc* 44(3):865–873. <https://doi.org/10.13225/j.cnki.jccs.2018.6039>
- Sun CL, Li GC, Gomah ME, Xu JH, Rong HY (2021) Experimental investigation on the nanoindentation viscoelastic constitutive model of quartz and kaolinite in mudstone. *Int J Coal Sci Technol* 8(5):925–937. <https://doi.org/10.1007/s40789-020-00393-2>
- Tan YL, Fan DY, Liu XS, Song SL, Li XF, Wang HL (2019) Numerical investigation of failure evolution for the surrounding rock of a super-large section chamber group in a deep coal mine. *Energy Sci Eng* 7(6):3124–3146. <https://doi.org/10.1002/ese3.484>
- Tan YL, Yu FH, Ma CF, Zhang GS, Zhao W (2021) Research on collaboration control method of bolt/cable-surrounding rock deformation in coal roadway with weakly cemented soft rock. *Coal Sci Technol* 49(1):198–207. <https://doi.org/10.13199/j.cnki.cst.2021.01.015>
- Tarifard A, Gorog P, Torok A (2022) Long-term assessment of creep and water effects on tunnel lining loads in weak rocks using displacement-based direct back analysis: an example from north-west of Iran. *Geomech Geophys Geoenergy Geosour* 8(1):37. <https://doi.org/10.1007/s40948-022-00342-0>
- Torabi-Kaveh M, Mehrnahad H, Morshedi S, Jamshidi A (2022) Investigating the durability of weak rocks to forecast their long-term behaviors. *Bull Eng Geol Environ* 81(1):8. <https://doi.org/10.1007/s10064-021-02504-y>
- Wang X (2022) Study on the floor heave mechanism and control technology of soft rock coal mining roadway. *J Shanxi Datong Univ (nat Sci Ed)* 38(1):98–102
- Wang JB, Liu XR, Song ZP, Zhao BY, Jiang B, Huang TZ (2018) A whole process creeping model of salt rock under uniaxial compression based on inverse S function. *Chin J Rock Mech Eng* 37(11):2446–2459. <https://doi.org/10.13722/j.cnki.jrme.2018.0670>
- Wang JF, Liu YK, Yang C, Jiang WM, Li Y, Xiong YQ (2022) Modeling the viscoelastic behavior of quartz and clay minerals in shale by nanoindentation creep tests. *Geofluids*. <https://doi.org/10.1155/2022/2860077>
- Xie HP, Wu LX, Zheng DZ (2019) Prediction on the energy consumption and coal demand of China in 2025. *J China Coal Soc* 44(7):1949–1960. <https://doi.org/10.13225/j.cnki.jccs.2019.0585>
- Xiong YL, Ye GL, Zhu HH, Zhang S, Zhang F (2017) A unified thermo-elasto-viscoplastic model for soft rock. *Int J Rock Mech Min* 93:1–12. <https://doi.org/10.1016/j.ijrmms.2017.01.006>
- Yang T, Xu C, Wang BX, Zhang L, Liao GH (2007) The cohesive strength and the friction angle in rock-soil triaxial rests. *China Min Mag* 12:104–107
- Ye GL, Nishimura T, Zhang F (2015) Experimental study on shear and creep behaviour of green tuff at high temperatures. *Int J Rock Mech Min* 79:19–28. <https://doi.org/10.1016/j.ijrmms.2015.08.005>
- Yin HJ, Guo GL, Li HZ, Wang TN, Yuan YF (2022) Prediction method and research on characteristics of surface subsidence due to mining deeply buried Jurassic coal seams. *B Eng Geol Environ* 81(10):449. <https://doi.org/10.1007/s10064-022-02946-y>
- Zhang XD, Li J, Hu XF, Hu YL, Qu Z (2018) Study of frozen Eolian soil loading model and experiment considering damage characteristic. *J Disaster Prev Mitig Eng* 38(1):7–13. <https://doi.org/10.13409/j.cnki.jdpme.2018.01.002>
- Zhao HZ, Tian Y, Guo QY, Li MJ, Wu JW (2020) The slope creep law for a soft rock in an open-pit mine in the Gobi region of Xinjiang, China. *Int J Coal Sci Technol* 7(2):371–379. <https://doi.org/10.1007/s40789-020-00305-4>
- Zhou Y (2022) Study on stability and control technology of tunnel surrounding rock in weak cementation and extremely soft stratum. Dissertation, University of Science and Technology Beijing.
- Zhou CY, Yu L, You FF, Liu Z, Liang LH, Zhang LH (2020) Coupled seepage and stress model and experiment verification for creep behavior of soft rock. *Int J Geomech* 20(9):04020146. [https://doi.org/10.1061/\(asce\)gm.1943-5622.0001774](https://doi.org/10.1061/(asce)gm.1943-5622.0001774)
- Zhu QW, Li TC, Zhang H, Ran JL, Li H, Du YT, Li WT (2022) True 3D geomechanical model test for research on rheological deformation and failure characteristics of deep soft rock roadways. *Tunn Undergr Space Technol* 128:104653. <https://doi.org/10.1016/j.tust.2022.104653>

Publisher's Note Springer Nature remains neutral with regard to jurisdictional claims in published maps and institutional affiliations.